Scientific Research and Essays Vol. 5(24), pp. 3850-3864, 18 December, 2010
Available online at http://www.academicjournals.org/SRE
ISSN 1992-2248 ©2010 Academic Journals

Full Length Research Paper

Fractional and structural characterization of organosolv and alkaline lignins from *Tamarix austromogoliac*

Yong-Chang Sun[1], Jia-Long Wen[1], Feng Xu[1] and Run-Cang Sun[1,2]*

[1]Institute of Biomass Chemistry and Technology, Beijing Forestry University, Beijing 100083, China.
[2]State Key Laboratory of Pulp and Paper Engineering, South China University of Technology, Guangzhou 510640, China.

Accepted 23 June, 2010

A comparative study was conducted on the seven lignin fractions, isolated from dewaxed *Tamarix austromogoliac* (TA) with DMSO, 70% ethanol containing 5% triethylamine, 70% ethanol containing 0.5% NaOH at 70°C for 5 h, and 1 M KOH, 1 M NaOH, 1 M LiOH and 1 M $NH_3 \cdot H_2O$ at 50°C for 5 h, respectively. The comprehensive structural characterization of the three organic solvent-soluble and four alkali-soluble lignin isolations were examined by UV, FT-IR, TGA, ^1H, ^{13}C and 2D ^{13}C-^1H correlation (HSQC) NMR spectroscopy techniques. The results showed that the DMSO-soluble lignin fraction, which was rich in hemicelluloses, had a relatively higher molecular weight (4730 g/mol) while the other six lignin isolations had lower molecular weights ranging from 1240 - 2160 g/mol. The thermogravimetric analysis (TGA) showed a decrease of thermal stability with a decrease in the molecular weight. In addition, the HSQC spectrum of the fraction isolated with 70% ethanol containing 0.5% NaOH from TA indicated a predominance of β-*O*-4′ aryl ether linkages (73% of total side chains), followed by lower amounts of β-β′ resinol-type linkages (19% of total side chains), trace amounts of β-5′ phenylcoumaran (3%), β-1′ spirodienone-type (3%) substructures and cinnamyl end groups (2%).

Key words: Organosolv lignins, *Tamarix austromogoliac*, TGA, ^{13}C NMR, HSQC.

INTRODUCTION

Tamarix austromogoliac (TA) is one of the main shrubs and has been planted in the desert regions in the northwest of China and Mongolia since the 1960s to prevent wind erosion and control desertification (Zhang et al., 2003). The shrubs not only have a great importance for reforestation of deserts and dry steppes, but also provide fuel, fodder, useful chemical components etc. (Zhang and Zhao, 1989; Saïdana et al., 2008). The utilization of these shrubs have shown the potential for a variety of applications such as bio-ethanol production and papermaking, moreover, these renewable forestry residues would be of great importance as materials, not only as a solution to the growing environmental threat, but as a solution to the uncertainty of petroleum supply (Mohanty et al., 2002).

Lignins are amorphous, three-dimensional plant copolymers essential for mechanical support, defense and water transport in vascular terrestrial plant, which linked through ether, aryl and carbon-carbon bonds such as β-*O*-4′, 4-*O*-5′, β-β′, β-1′, β-5′ and 5-5′. They are usually derived from three hydroxycinnamyl alcohols (the monolignols: p-coumaryl, coniferyl and sinapyl alcohols) by a dehydrogenating polymerization involving radical coupling (Sederoff et al., 1999). However, the amount of lignin in plants varied widely due to the low degree of order and the high degree of heterogeneity in its structure. In gymnosperms, for example, lignin is mainly polymerized from *p*-coumaryl alcohol and coniferyl alcohol, with coniferyl alcohol being predomainant (-90%). In wood angiosperms, lignin is derived from coniferyl alcohol and sinapyl alcohol in roughly equal

*Corresponding author. E-mail: xfx315@bjfu.edu.cn, rcsun3@bjfu.edu.cn. Tel/Fax: +86-10-62336972.

proportions. In addition, lignin *in situ* has no structural regularity; along with the some 20 different types of bonds present within the lignin itself, lignin seems to be particularly associated with hemicellulosic polysaccharides (Sun et al., 2000b). This makes it very difficult to use degradative methods for structural determination. Because of its polyphenolic chemical structure, lignin can be used in manufacturing adhesives, epoxi- and phenolic- resins, and polyolefins as well as in a variety of nonspecific and novel applications. Lignin isolated from wood or other lignocellulosic biomass is commercially available and is used in high-value-added chemicals.

It is well known that nuclear magnetic resonance (NMR) spectroscopy is one of the most widely used methods for the detailed structural characterization of lignin (Zhang and Gellerstedt, 2007). Because of overlapping signals from different lignin moieties, in addition, isolations of lignins, containing carbohydrate and protein impurities, it is hard to analyse lignin structure using 1D NMR. However, advanced ^{1}H-^{13}C correlation 2D NMR spectroscopic technique, heteronuclear single quantum correlation (HSQC) sequence, is a powerful tool for qualitative and quantitative analysis of lignin structure (Martínez et al., 2008; Rencoret et al., 2009a). It provides resolution of signals overlapping in the ^{1}H and ^{13}C NMR spectra and reveals both the aromatic units and the different inter-unit linkages present in lignin. The HSQC sequence gives information about the correlation between ^{1}H and ^{13}C atoms via one boud coupling ($^{1}J_{CH}$). Hence, various inter-unit bonds such as several types of ether (β-*O*-4′, 4-*O*-5′) and carbon-carbon linkages can be identified. This study's show here that the HSQC spectrum gives reliable estimates for the structural features, such as the relative abundance of β-*O*-4′ inter-unit linkages, and signals observed at 63.5/4.0 and 4.1 ppm corresponding to the C_{γ}-H_{γ} correlations in γ-acetylated lignin units. These signals indicate that the lignin from TA is partially acetylated at the γ-carbon of the side chain. In this study, the isolated lgnins were characterised by both degradation methods such as oxidation and thermal analysis, and nondestructive techniques, e.g., Ultraviolet (UV), Fourier transform infrared (FT-IR), carbon-13 nuclear magnetic resonance (^{13}C NMR) spectroscopy and gel permeation chromatography (GPC).

MATERIALS AND METHODS

Materials

T. austromogoliac, 5 years old, was harvested in October 2009 in Mongolia, China, the leaves and the bark were removed, and the stalks were chipped into small pieces. After drying at 60°C for 16 h in an oven, the chips were then grounded to pass a 40 - 60 mm size screen, and the powder was dewaxed with toluene-ethanol (2:1, v/v) in a Soxhlet instrument for 6 h. The dewaxed sample was further dried in a cabinet oven with air circulation at 60°C for 16 h and stored in a desiccator under vacuum before extraction with different solvents. The major composition (%, w/w) of TA is cellulose 39.8%, hemicellulose 31.0% and lignin 19.8% on a dry weight basis, determined by the method for measuring the chemical composition of wheat straw described previously (Lawther et al., 1995).

Methods

Fractional isolation of lignins

The lignins were fractionated according to the scheme in Figure 1. The extractive-free powder (3 g) was treated with DMSO, 70% ethanol containing 5% triethylamine, 70% ethanol containing 0.5% NaOH at 70°C for 5 h, and 1 M KOH, 1 M NaOH, 1 M LiOH and 1 M $NH_3{\cdot}H_2O$ at 50°C for 5 h, respectively, with a solid to liquid ratio of 1:25 (g/ml). The resulting suspension was filtered, and the residue was washed with 70% ethanol on a nylon cloth. Each of the combined supernatant was adjusted to pH 5.5 - 6 with 6 M acetic acid and concentrated on a rotary evaporator under reduced pressure to about 30 ml, The released hemicelluloses were then precipitated by pouring the concentrated filtrate into 3 volumes of 95% ethanol (2 h, 25°C), and the isolations were washed with 70% ethanol at room temperature and freeze-drized. The solubilized lignins were obtained from the corresponding supernatants by re-precipitation at pH 1.5 - 2.0 after separation of hemicellulosic fractions. The isolated lignins were purified by washing with acidified water (pH 2.0) at room temperature and freeze-drized. Note that the fractions 1 (L_1), 2 (L_2) and 3 (L_3) represent the lignin isolations extracted with DMSO, 70% ethanol containing 5% triethylamine and 70% ethanol containing 0.5% NaOH, respectively. The fractions 4 (L_4), 5 (L_5), 6 (L_6) and 7 (L_7) represent the lignin fractions extracted from TA with 1 M KOH, 1 M NaOH, 1 M LiOH and 1 M $NH_3{\cdot}H_2O$, respectively.

Characterization of lignin fractions

In this study, the monomeric composition of the non-condensed units of the seven lignin fractions was characterized by alkaline nitrobenzene oxidation. The phenolic aldehydes and acids were analyzed by high-performance liquid chromatography (HPLC) as previously reported (Sun et al., 2001).

The weight-average ($\bar{M}_w$) and number-average ($\bar{M}_n$) molecular weights of the lignin fractions were determined by gel permeation chromatography with a refraction index detector (RID) on a PL-gel 10 µm Mixed-B 7.5 mm ID column. The hemicellulosic moieties associated with lignin fractions were determined by hydrolyzing with dilute sulfuric acid. The experiments were performed at least in duplicate, and the average value calculated for all of the lignin fractions. Ultraviolet-visible (UV-vis) spectra were recorded on a Techcomp UV2300 array spectrophotometer. The FT-IR spectra of the lignin fractions were recorded from a KBr disc containing 1% finely ground samples on a Tensor 27 FT-IR spectrophotometer in the range of 4000 - 400 cm^{-1} as previously reported (Yuan et al., 2009).

The solution-state ^{1}H and ^{13}C NMR spectra were obtained on a Bruker AVIII 400 MHz spectrometer operating in the FT mode at 100.6 MHz. The lignin samples (25 mg for ^{1}H, 180 mg for ^{13}C) were dissolved in 1 ml of deuterated dimethylsulfoxide (DMSO-d_6, 99.8% D). The ^{1}H–NMR spectrum was recorded at 25°C after 128 scans. A 30° pulse flipping angle, a 13.6 µs pulse width, a 3.98 s acquisition time, and 1 s relaxation delay time were used. The ^{13}C NMR spectrum was recorded at 25°C after 30,000 scans. A 30° pulse flipping angle, a 9.2 µs pulse width, a 1.67 s acquisition time, and 2 s relaxation delay time were used. ^{1}H-^{13}C correlation 2D (HSQC) NMR spectrum was also recorded at 25°C on a Bruker

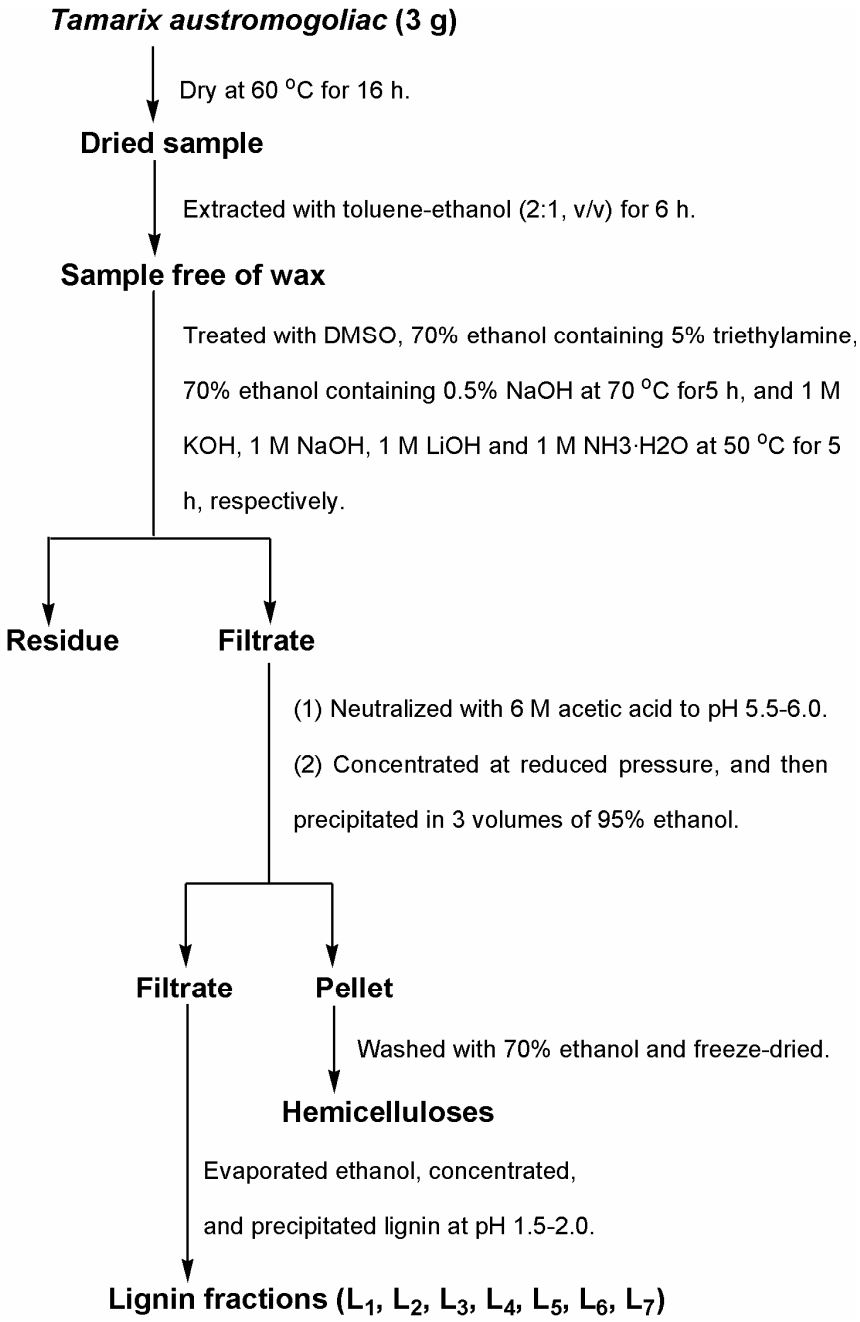

Figure 1. Scheme for isolation of lignins from *T. austromogoliac*.

AVIII 400 MHz spectrometer equipped with a z-gradient double resonance probe. Around 25 mg sample was dissolved in 1 ml of and 20,000 Hz for the ^{1}H- and ^{13}C- dimensions, respectively. The number of collected complex points was 1024 for ^{1}H-dimension with a relaxation delay of 1.5 s. The number of scans was 128 and 256 time increments were always recorded in ^{13}C-dimension. The $^{1}J_{CH}$ used was 145 Hz. Prior to Fourier transformation, the data matrixes were zero, filled up to 1024 points in the ^{13}C-dimension.

Thermal analysis of the lignin samples were performed using thermogravimetric analysis (TGA) and differential thermal analysis (DTA) on a simultaneous thermal analyzer (DTG-60, Shimadzu, Japan). This apparatus was continually flushed with nitrogen. The sample weighed approximately 8 - 15 mg and heated in an deuterated dimethylsulfoxide (DMSO-d_6) and 2D NMR spectrum was recorded in HSQC experiment. The spectral widths were 8000 aluminium crucible from room temperature to 600℃ at a rate of 10℃/min.

RESULTS AND DISCUSSION

Yield and purity of lignin

The yield of lignin fractions and the extraction conditions are presented in Table 1. As the data show, extraction

Table 1. Extraction conditions and yield of lignin (% based on the amount of Klason lignin in the starting wood, w/w) solubilized from the extractive-free *T. austromogoliac*.

Lignin fraction	Extractant	Temperature (°C)	Reaction time (h)	Yield (%)
L_1	DMSO	70	5	61.7
L_2	70% ethanol containing 5% triethylamine	70	5	14.6
L_3	70% ethanol containing 0.5% NaOH	70	5	27.4
L_4	1 M KOH	50	5	11.4
L_5	1 M NaOH	50	5	11.2
L_6	1 M LiOH	50	5	13.1
L_7	1 M $NH_3 \cdot H_2O$	50	5	3.4

Table 2. The yield (% lignin sample, w/w) of neutral sugars and uronic acids in the isolated lignin fractions.

Netural sugars/uronic acids	Lignin fraction**						
	L_1	L_2	L_3	L_4	L_5	L_6	L_7
Arabinose	0.17	0.86	0.22	1.43	0.27	0.14	0.64
Rhamnose	0.06	0.07	ND*	ND*	0.03	ND*	0.13
Galactose	0.09	0.48	0.05	0.02	0.04	0.05	0.38
Glucose	5.42	1.44	0.19	0.18	0.30	0.61	1.26
Mannose	0.05	0.24	0.09	ND*	ND*	0.07	ND*
Xylose	0.57	0.10	0.22	0.35	2.26	0.12	2.91
Uronic acids	0.21	0.15	0.02	0.03	0.22	0.04	0.42
Total	6.58	3.35	0.79	2.00	3.22	1.02	5.74

**Corresponding to the acid-insoluble lignin fractions in Table 1; *ND, not detected.

with DMSO, 70% ethanol containing 5% triethylamine, 70% ethanol containing 0.5% NaOH, 1 M KOH, 1 M NaOH, 1 M LiOH and 1 M $NH_3 \cdot H_2O$ released 61.7, 14.6, 27.4, 11.4, 11.2, 13.1 and 3.4% of the original lignin (% based on the amount of Klason lignin in the starting wood, w/w), respectively. In comparsion, the DMSO-soluble fraction had a highest yield, while the $NH_3 \cdot H_2O$-soluble fraction released only 3.4% of the original lignin.

The content of natural sugars and uronic acids in the seven lignin fractions indicated that all the lignin fractions contained small amounts of associated hemicelluloses (Table 2). Xylose (0.57% in L_1, 0.10 - 2.91% in L_2-L_7), arabinose (0.14 - 1.43% in L_1-L_7), glucose (5.42% in L_1, 0.18 - 1.44% in L_2-L_7) were identified as the major sugars. Rhamnose and mannose appeared in trace. From fraction 1 - 7, the hemicelluloses associated to lignin fractions amounted to 6.58, 3.35 0.79, 2.00, 3.12, 1.02 and 5.74%, respectively. Clearly, fraction L_1 and L_7 contained relatively noticeable amounts of associated hemicelluloses, whereas, fractions L_3, L_4 and L_6 contained minor amounts of bound hemicelluloses, ranging from 0.79 - 2.00%. This may explain the cleavage of linkages between lignin and hemicelluloses during the treatments by 70% ethanol containing 0.5% NaOH, 1 M KOH and 1 M LiOH, such as ester bonds between ferulic acid and hemicelluloses or between *p*-coumaric acid and lignin and α-aryl ether linkages between lignin and hemicelluloses. The xylose content of the DMSO-soluble lignin fraction L_1, NaOH-soluble lignin fraction L_5 and $NH_3 \cdot H_2O$-soluble lignin fraction L_7 were slightly higher as compared to that of the other lignin fractions. The higher xylose content of fractions L_1 and L_7 implied that the lignin-hemicellulose linkages did not significantly cleaved under the conditions given in Table 1, while the higher xylose content of fraction L_5 needs to be verified further. Furthermore, a large amount of glucose found in the hydrolysate of DMSO-soluble lignin fraction L_1 arose potentially from the degradation of hemicelluloses or β-glucan under the condition used, since the glucose liberated was partially attributed to the hemicelluloses fraction.

Composition of phenolic acids and aldehydes

Alkaline nitrobenzene oxidation is a destructive technique that depolymerizes the lignin by cleavage of ether linkages and oxidation of three constitutive monomeric lignin units guaiacyl (G), syringyl (S) and *p*-hydroxyphenyl (H), which produce the corresponding vanillin, syringaldehyde and *p*-hydroxybenzaldehyde, respectively (Sun et al., 2001). In this case the differences in the structure of the fractions would be observed. The results of the relatively yields of the

Table 3. The yield (relative mol %) of phenolic acids and aldehydes from alkaline nitrobenzene oxidation of the acid-insoluble lignin fractions.

Phenolic acid and aldehydes	Lignin fraction*						
	L_1	L_2	L_3	L_4	L_5	L_6	L_7
p-Hydroxybenzoic acid	2.4	2.7	0.6	0.6	1.0	1.0	2.1
p-Hyroxybenzaldehyde	17.2	10.3	4.8	9.2	7.6	1.3	12.0
Vanillic acid	13.4	10.3	16.4	9.1	8.7	1.0	7.8
Vanillin	29.3	39.7	58.9	55.8	55.6	62.7	43.4
Syringic acid	10.1	15.1	9.7	12.7	13.5	16.0	11.3
Syring aldehyde	21.5	16.8	6.3	8.0	8.2	6.6	14.8
Acetovanillone	0.7	0.8	0.2	1.0	0.3	0.8	2.1
Acetosyringone	0.4	0.8	0.3	0.8	0.4	1.0	1.2
p-Coumaric acid	0.7	1.9	0.2	0.2	0.3	0.8	0.4
Ferulic acid	4.5	1.4	2.8	2.5	4.5	9.0	5.0
G/S	1.4:1	1.6:1	4.7:1	3.0:1	2.9:1	2.7:1	2.0:1
(G/S/H)**	2.2:1.6:1	2.5:3.9:1	14.0:3.0:1	6.7:2.2:1	7.5:2.6:1	25.8:10.4:1	3.8:1.9:1

**G represents the relatively total moles of vanillin, vanillic acid and acetovanillone; S represents the relatively total moles of syringaldehyde, syringic acid and acetosyringone; and H represents the relatively total moles of *p*-hydroxybenzaldehyde and *p*-hydroxybenzoic acid. *Corresponding to the acid-insoluble lignin fractions in Table 1.

phenolic acids and aldehydes in each of the fraction are listed in Table 3, and can be used to derive information about the composition of the original polymer (Billa et al., 1996). The relatively higher oxidation products were found to be vanillin, syringaldehyde and syringic acid, which accounted for 69.5 - 85.3% of the total phenolic monomers, resulted from the degradation of non-condensed guaiacyl units and non-condensed syringyl units, respectively. In general, lower molecular weight of lignin fractions contained more uncondensed groups and was capable of being oxidized. Similar results have been reported by Rakhmatullaev et al. (1979). The presence of less *p*-hydroxybenzoic acid (0.6 - 2.7%) was considered to be most likely indicative of *p*-hydroxycimmamyl of *p*-coumaryl alcohol in the lignin fraction. A higher content of *p*-hydroxybenaldehyde (17.2%) obtained in fraction L_1 was presumed to be largely due to the partial oxidation of *p*-coumaric acid by nitrobenzene, since *p*-hydroxybenaldehyde resulted partly from *p*-coumaric acid oxidation (Scalbert et al., 1986).

There are significant differences in the chemical structure of lignin depending on its morphological origin (Önnerud and Gellerstedt, 2003). These differences can be elucidated by the ration of different G/S. The molar ratios of G (the relative total mol of vanillin, vanillic acid and acetovanillone) to S (the relative total mol of syringaldehyde, syringic acid and acetosyringone) in the seven lignin oxidation products were 1.4:1 in L_1, 1.6:1 in L_2, 4.7:1 in L_3, 3.0:1 in L_4, 2.9:1 in L_5, 2.7:1 in L_6 and 2.0:1 in L_7, indicating a relatively increase of G/S from fraction L_1 to L_2 and to L_3, and decrease from L_4 to L_5 to L_6 and to L_7. A higher content of total relative mol of G (64.5 - 66%, fraction L_4-L_6) units revealed that the non-condensed β-aryl ether linked guaiacyl units, isolated with alkali were more easily degradable than non-condensed β-aryl ether linked syringyl units in TA cell walls. This result was consistent with the studies on wheat straw alkaline lignins by Sun et al. (1997).

UV spectra

UV spectroscopy has been used to semiquantitatively determine the purity of lignin or monitor the lignin distribution among various tissues of gymnosperm and dicotyledonous angiosperm with respect to the concentration (Sun et al., 2001). The spectra of L_1, L_4 and L_6 fractions are shown in Figure 2. Clearly, all the spectra exhibited the basic UV spectrum typical of lignin with a maximum at 274 or 276 and 330 nm. The first absorption maximum was originated from non-condensed phenolic groups (aromatic ring) in lignin. The presence of a second characteristic region around 330 nm indicated that the lignin fraction L_4, isolated with 1 M KOH, contained higher amounts of hydroxycinnamic acids such as ferulic and *p*-coumaric acids (Scalbert et al., 1985, 1986). As can be seen from those spectra, the absorption coefficient showed a decrease from spectrum L_1 (DMSO-soluble) to L_4 (1 M KOH-soluble) and to L_6 (1 M LiOH-soluble). In comparison with fraction L_1, the lower absorption coefficients of fractions L_4 and L_6 were probably due to the associated non-lignin materials, such as ash and salt. This is in agreement with the results obtained by Sun et al. (2000a). The shift of the maximum wavelength from 276 (fraction L_6) to 274 nm (fraction L_1) suggested a slighter higher content of syringyl units in lignin fraction L_1 than that in fraction L_6, because S units exhibit the bands at somewhat shorter wavelengths.

Molecular mass

The question of whether the different treatments caused

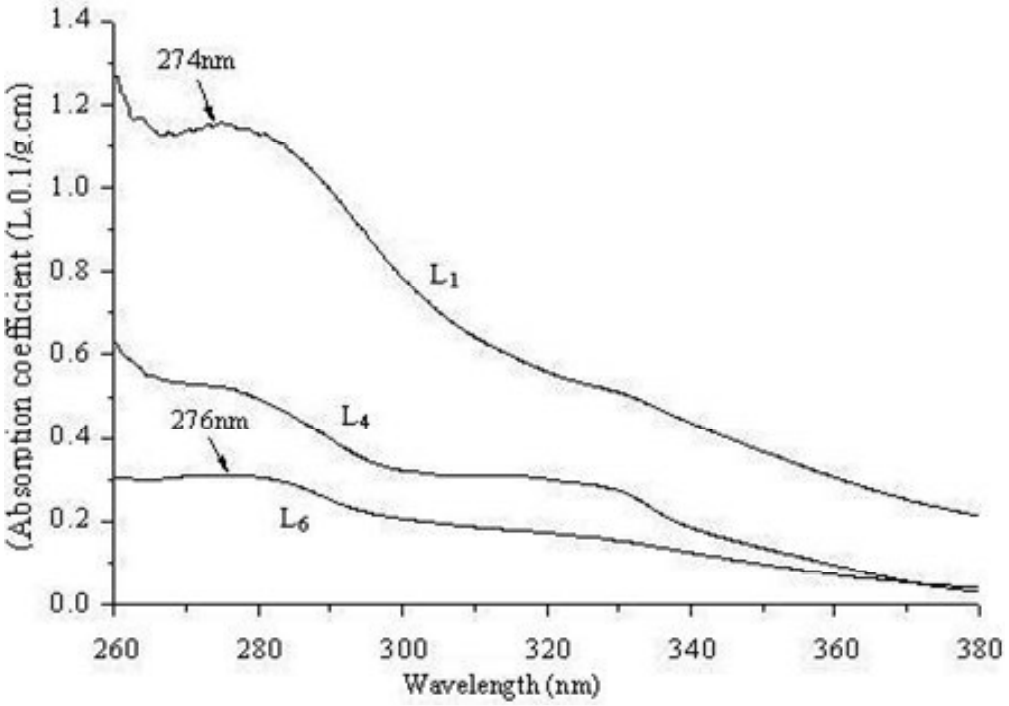

Figure 2. UV spectra of three acid-insoluble lignin fractions: L_1, L_4 and L_6.

Table 4. Weight-average ($\bar{M}_w$) and number-average ($\bar{M}_n$) molecular weights and polydispersity ($\bar{M}_w$ / $\bar{M}_n$) of the acid-insoluble lignin fractions.

	Lignin fraction*						
	L_1	L_2	L_3	L_4	L_5	L_6	L_7
$\bar{M}_w$	4730	1585	2160	2010	1850	1400	1240
$\bar{M}_n$	530	1040	940	1100	1020	780	820
$\bar{M}_w$ /$\bar{M}_n$	8.9	1.5	2.3	1.8	1.8	1.8	1.5

*Corresponding to the acid-insoluble lignin fractions in Table 1.

some lignin depolymerization was addressed by the investigation of the GPC elution curves for the seven lignin fractions. The weight-average ($\bar{M}_w$) and number-average ($\bar{M}_n$) molecular weights and polydispersity ($\bar{M}_w/\bar{M}_n$) of the acid-insoluble lignin samples are given in Table 4. From these data, a much higher molecular weight was found for L_1 ($\bar{M}_w$, 4730 g/mol), medium molecular weights for fractions L_3 - L_5 ($\bar{M}_w$, 1850 - 2160 g/mol), and lower molecular weights for L_2, L_6 and L_7 ($\bar{M}_w$, 1240-1585 g/mol).

It is clear that lignin released during the DMSO treatment did not cause significant depolymerization on the lignin macromolecular structure. However, the elution profiles declared a very broad distribution of molecular size as indicated by its polydispersity ($\bar{M}_w/\bar{M}_n$) value of 8.9. While the molecular weight-average ($\bar{M}_w$) of fractions L_3 - L_5 was nearly constant, which were treated with 70% ethanol containing 0.5% NaOH, 1M KOH and 1 M NaOH, respectively. This phenomenon suggested that the lignin polymers were substantially degraded under the alkaline conditions used. On the other hand, the lower weight-average ($\bar{M}_w$) molecular weight of lignin fraction L_7 was probably due to weak alkaline extraction, which released only lower molecular materials. It's well known that β-*O*-4′ ether bond is the most common linkage in all lignin types, however, some quantities of carbon-carbon bonds between the lignin units involving C-5 of the aromatic ring, are the most abundant (Brunow et al., 1999). G-type units are able to form this kind of bond, and these

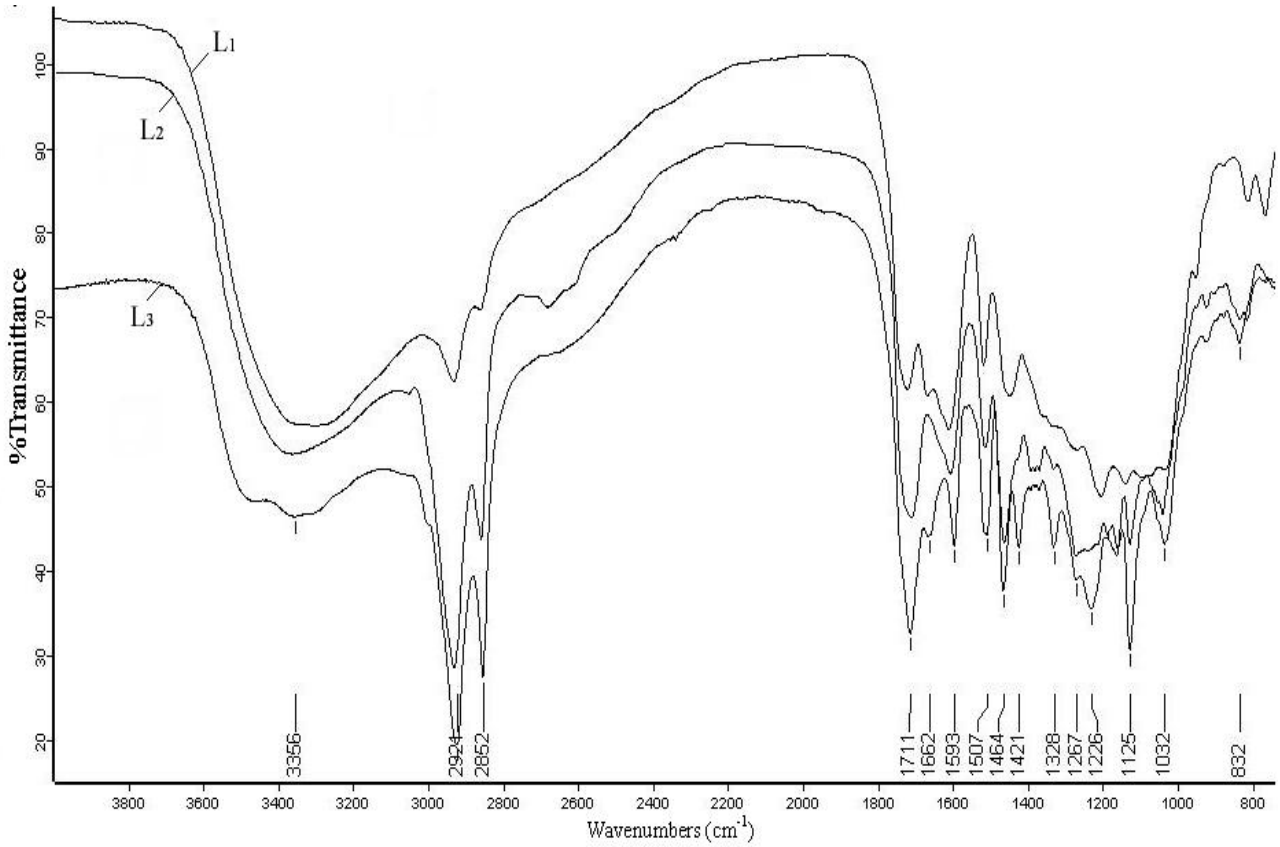

Figure 3. FT-IR spectra of *T. austromogoliac* lignin fractions isolated with DMSO (spectrum 1), 70% ethanol containing 5% triethylamine (spectrum 2) and 70% ethanol containing 0.5% NaOH (spectrum 3) at 70℃ for 5 h.

C-C bonds are not cleaved during conditions such as different alkalis because of their higher stability. Lignins strictly composed of G units are expected to have a higher molecular weight than those presenting higher contents of S units (Tejado et al., 2007). This is in agreement with the result of the alkaline nitrobenzene oxidation. Furthermore, the results present in Table 4 showed that all the fractions except for fraction L_1 have a relatively narrow distribution of molecular weight, and the polydispersity ($\bar{M}_w/\bar{M}_n$) values take on a decreased trend, which decreased from 2.3 of fraction L_3 to 1.5 of fraction L_7, as well as the decreasing tendency of molecular weights from 2160 g/mol of fraction L_3 to 1240 g/mol of fraction L_7.

FT-IR spectra

The FT-IR spectra of the DMSO-soluble lignin fraction L_1, ethanol triethylamine-soluble lignin fraction L_2 and alkaline ethanol-soluble lignin fraction L_3 are illustrated in Figure 3. As can be see from the spectra, the three lignin fractions have similar FT-IR spectra, the relative intensities of the bands for aromatic skeleton vibrations, assigned at 1594 or 1593, 1507 and 1421 or 1422 cm^{-1} (Figures 3 and 4) are rather similar, indicating a similar structure of the lignin fractions. These typical spectra of lignin revealed that the “core” of the lignin structure did not change significantly during the treatment with organic solvents and alkaline treatment processes. However, the changes in the carbonyl absorption region might enable the evaluation of the effects of various treatments. The bands at 1662 or 1663 cm^{-1} and 1711 or 1710 cm^{-1} are assigned to the presence of conjugated and nonconjugated carbonyl groups in the lignin structure (Sun et al., 2005). The ring breathing with C-O stretching is assigned at 1328, 1267 and 1226 cm^{-1}. Clearly, the spectrum of fraction L_3 is typified by a strong absorption at 1711 cm^{-1}, while this band is rather weak in the spectrum L_1. This result implies that a noticeable oxidation of the lignin structure did occur during the extraction with 70% ethanol containing 0.5% NaOH. A wide absorption band focused at 3356 and 3364 cm^{-1} is originated from O-H stretching vibration in aromatic and aliphatic OH groups, whereas, bands at 2921-2926 cm^{-1}, 2852 cm^{-1} and at 1464cm^{-1} arise from the C-H stretching and asymmetric vibrations of CH_3 and CH_2, respectively (Tejado et al., 2007).

It is well known that in softwoods the lignin network is mainly composed of G moieties with small amounts of

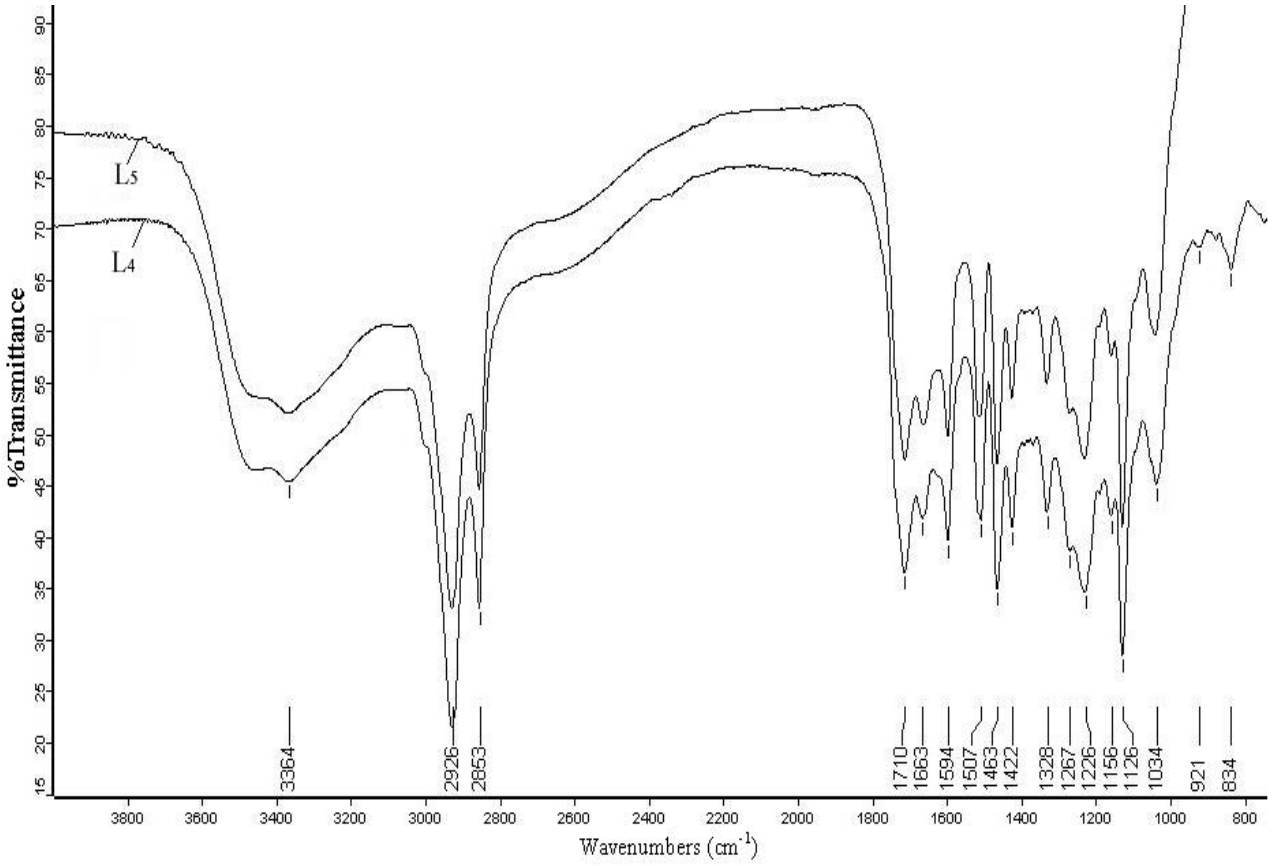

Figure 4. FT-IR spectra of *T. austromogoliac* lignin fractions isolated with 1 M KOH (spectrum 4) and 1 M NaOH (spectrum 5) at 50 °C for 5 h.

S and only traces of H-type unit (Boeriu et al., 2004). On the other hand, in hardwoods and dicotyl crops, different G/S ratios have been reported. These characteristics become visible in the spectra of the three studied lignin fractions L_1, L_2 and L_3. As can be seen from Figure 3, the absorptions at 1328 and 1125 cm^{-1} are due to the syringyl units in lignin molecules, while the bands at 1267, 1226 and 1032 cm^{-1} belong to guaiacyl units in the lignin molecules. The intensity ratios of 1507 - 1464 cm^{-1} increased from L_1 to L_2 to L_3, indicating that fraction L_3 has a relatively higher content of G units than the fractions L_1 and L_2. These results supported those obtained by alkaline nitrobenzene oxidation, in which the relative molar ratio of G/S in the three lignin fractions are 1.4:1, 1.6:1 and 4.7:1, respectively.

The noticeable higher absorption at 1032 cm^{-1} of L_3 (Figure 4) owing to the C-O stretching vibration in the guaiacyl units (Tejado et al., 2007), indicated more G units in the lignin fraction L_3, isolated with 70% ethanol containing 0.5% NaOH. The spectra of L_4 and L_5 are rather similar, indicating a similar structure of the lignin fractions, released during the treatment with 1 M KOH and 1 M NaOH, respectively. In addition, aromatic C-H out of plane bending appears at 832 or 834 cm^{-1}.

^{1}H, ^{13}C and 2D NMR spectra

The chemical structure of lignin fraction L_3 was investigated with ^{1}H, ^{13}C and 2D NMR spectrometry, and their spectra are shown in Figures 5, 6 and 7. The integrals of signals between 6.0 and 8.0 ppm (Figure 5) are attributed to the aromatic protons in G and S units, whereas, those between 0.8 and 1.5 ppm are attributed to aliphatic moiety in the lignin fractions (Tejado et al., 2007). In particular, the signals at 6.7 and 6.8 ppm represent the aromatic protons in G units, while 6.6 ppm is originated from the S units (Faix et al., 1992). A weak signal at 6.6 ppm reveals that the lignin fraction L_3, isolated with 70% ethanol containing 0.5% NaOH, contained only small amounts of S units, corresponding to the results obtained by alkaline nitrobenzene oxidation, as shown by a G/S ratio of 4.7:1. The peaks at 2.0, 2.1 and 2.2 ppm arise from the methyl protons adjacent to double bonds or carbonyl groups (Marchessault et al., 1981). Methoxyl protons ($-OCH_3$) give two strong signals at 3.4 and 3.7 ppm. A sharp signal at 2.5 ppm relates to the protons in DMSO. The peak at 5.3 ppm represents H_α in β-5' linkages, and the signal at 4.9 ppm represents H_α in β-*O*-4′ linkages

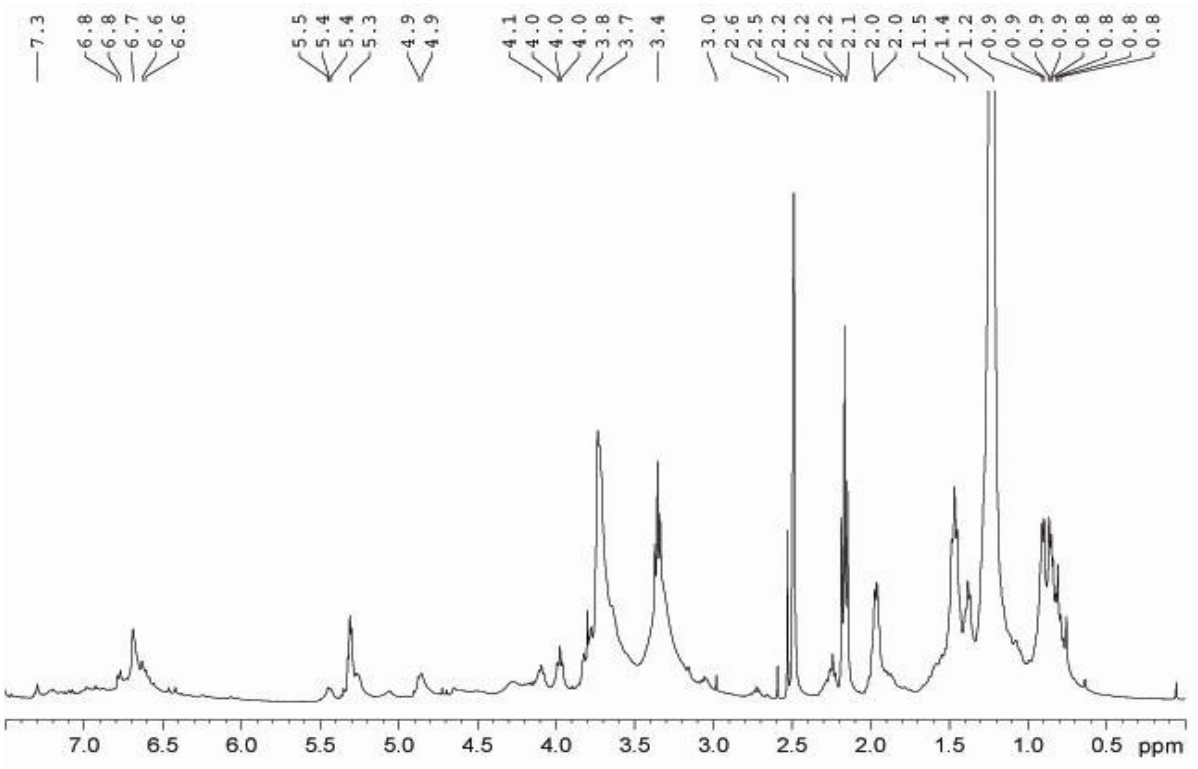

Figure 5. ^{1}H NMR spectrum of lignin fraction L_3 isolated with 70% ethanol containing 0.5% NaOH at 70°C for 5 h.

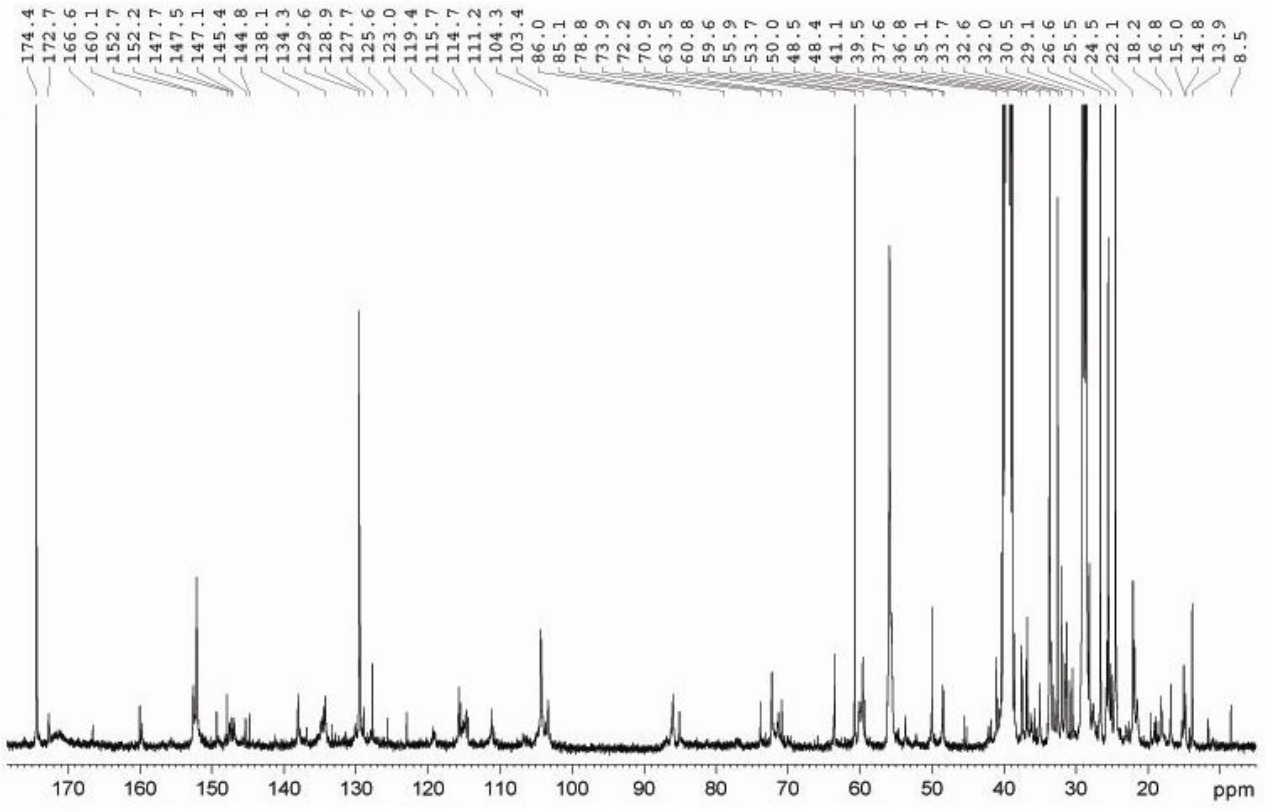

Figure 6. ^{13}C NMR spectrum of lignin fraction L_3 isolated with 70% ethanol containing 0.5% NaOH at 70°C for 5 h.

Table 5. Carbon chemical shifts (δ, ppm), intensity and assignments of the lignin preparation L_3 in ^{13}C NMR spectrum.

δ (ppm)	Intensity*	Assignment**	δ (ppm)	Intensity	Assignment
174.4	s	C-6 in methyl uronates	115.5	w	C-β, $P_β$
172.7	w	-COOH, aliphate	114.7	w	C-5, G
166.6	w	-COOH, conjugated	111.2	w	C-2, G
152.7	m	C-3/C-5, S	104.3	m	C-2/C-6, S
149.4	m	C-3, G etherified	86.0	w	C-β in β-*O*-4′
147.7	w	C-4, G etherified	85.1	w	C-α in β-β′
147.5	w	C-3/C-5, S nonetherified	73.9	w	C-3, Xyl internal unit
145.4	w	C-4, G nonetherified	72.2	w	C-α in β-*O*-4′
138.1	m	C-4, S etherified	70.9	w	C-γ in β-β′
134.3	w	C-1, G etherified, C-1, S etherified	63.5	m	C-γ in β-5′
129.6	s	C-2/C-6, PC ester	60.8	s	C-6 in 4-*O*-MeGlcA
128.9	w	C-α/C-β, Ar-CH=CH-CH_2OH	60.1	w	C-5′ α-L-arabinofuranosyl
127.7	w	C-2/C-6, H	59.6	w	C-γ in β-*O*-4′
125.6	w	C-5/C-5′, 5-5′ structures	55.9	s	OCH_3 in S and G unit
123.0	w	C-6, FE ether	55.6	w	OCH_3 in S and G unit
119.4	w	C-6, G	53.7	w	C-β in β-β′
115.7	w	C-3/C-5, P	20-33.7	s	α-, β-Methylene groups

**G, guaiacyl unit; S, syringyl unit; H, *p*-hydroxylphenyl unit; PC, *p*-coumaric acid; FE, ferulic acid; Xyl, xylose; 4-*O*-MeGlcA, 4-*O*-methylglucuronic acid. *s, strong; m, medium and w, weak.

(Lapierre et al., 1982). The signals in the region of 4.6 - 4.7 and 4.0 - 4.5 ppm are originated from $H_β$ and $H_γ$ of β-*O*-4′ structures, respectively (Lapierre et al., 1982). The small signal at 8.7 ppm is attributed to the C=O groups in aldehydes such as cinnamaldehyde and benzaldehyde structures.

^{13}C NMR spectroscopy is one of the most powerful tools in lignin chemistry. ^{13}C NMR spectrum of fraction L_3, isolated with 70% ethanol containing 0.5% NaOH is investigated (Figure 6), and their chemical shifts (δ, ppm), intensity, and assignment are listed in Table 5. In the region of carboxyl structure, the signal at 174.4 ppm, attributed to carbon in carbonyl groups, is originated from unconjugated aliphatic carboxyl groups (Tai et al., 1990), whereas, the signal at 166.6 ppm is probably dut to conjugated carboxyl structures. The small signal at 172.7 ppm resulted from the aliphatic carboxyl groups. In the region of the aromatic part of the lignin, G units were identified by signals at 149.4 and 148.0 (C-3, G etherified), 147.7, 147.5, 147.1 (C-4, G etherified), 145.4 and 144.8 (C-4, G nonetherified), 134.3 (C-1, G etherified), 119.4 (C-6, G), 114.7 (C-5, G) and 111.2 ppm (C-2, G). The S residues were verified by signals at 152.7 and 152.2 (C-3/C-5, S), 147.7, 147.5, 147.1 (C-3/C-5, S nonetherified), 138.1 (C-4, S etherified), 134.3 (C-1, S etherified) and 104.3 ppm (C-2/C-6, S). Signals corresponding to $C_{2,6}$-$H_{2,6}$ correlations in $C_α$-oxidized S units (S′ 106.3 and S″ 106.8 ppm) were also present in the HSQC spectrum (del Río et al., 2009). The H units were detected at 127.7 (C-2/C-6, H) and a sharp peak at 129.6 ppm (C-2/C-6 PC ester). The signal at 125.6 ppm is indicative of C-5/C-5′ in 5-5′ structures. The *p*-hydroxyphenyl units and *p*-coumarate ester give signals at 115.7 (C-3/C-5, P) and 115.5 ppm(C-β, $P_β$), respectively. The correlations above are in agreement with previous studies described by Xu et al. (2008). These signals indicated that the lignin fraction could be justified as GSH-type lignin, corresponding to the results of the G/S/H ratio obtained by nitrobenzene oxidation. The signals at 174.4 and 60.8 ppm represent C-6 in methyl uronates and the 4-O-methoxyl group of glucuronic acid residue, respectively (Xu et al., 2006). These two strong bands for uronic acids and esters suggested that the uronic acids are closely associated with lignin macromolecules in the cell wall of TA, which is in line with the results obtained by Xu et al. (2008). Etherified ferulic acid gives a weak signal at 123.0 ppm (C-6, FE ether). These observations implied that *p*-coumaric acid is associated to lignin by ester bonds, while ferulic acid is linked to lignin by ether bonds (Nimz et al., 1981). Besides, C-α/C-β in Ar-CH=CH-CH_2OH give a signal at 128.9 ppm.

The β-*O*-4′ structure was also revealed in the ^{13}C NMR spectrum. In Figure 6, the strong signals at 55.9 and 55.6 ppm represent OCH_3 in S and G units. Signals observed at 60.1 and 73.9 ppm corresponded to C-5 of α-L-arabinofuranosyl residue linked to β-D-xylans and C-3 in xylose internal unit, respectively (Izydorczyk and Biliaderis, 1995). This phenomenon confirmed again that hemicelluloses are associated with lignin in the cell walls of TA. The resonance of C-β, C-α and C-γ in β-*O*-4′ linkages gives signals at 86.0, 72.2 and 59.6 ppm, respectively. The common carbon-carbon linkages such as β-β′ (C-α 85.1, C-γ 70.9 and C-β 53.7 ppm) and β-5′

Table 6. Assignments of main lignin ^{13}C-^{1}H correlation signals in the HSQC spectrum shown in Figure 7.

Labels	δ_c / δ_H (ppm)	Assignment
B_β	53.7/3.1	C_β-H_β in β-β′ (resinol) substructures (B)
-OMe	55.9/3.8	C-H in methoxyls
A_γ	59.6/3.7 and 60.8/3.4	C_γ-H_γ in β-*O*-4′ substructures (A)
D_β	60.1/3.2	C_β-H_β in spirodienone substructures (D)
F_γ	61.5/4.08*	C_γ-H_γ in *p*-hydroxycinnamyl alcohol end groups (F)
A'_γ	63.5/4.0 and 4.1	C_γ-H_γ in γ-acetylated β-*O*-4′ substructures (A′)
B_γ	70.9/3.8 and 4.1	C_γ-H_γ in β-β′ (resinol) substructures (B)
A_α	72.2/4.9	C_α-H_α in β-*O*-4′ substructures linked to a S unit (A)
D_α	81.3/5.09*	C_α-H_α in spirodienone substructures (D)
B_α	85.1/4.7	C_α-H_α in β-β′ (resinol) substructures (B)
Ae_β(S)	86.0/4.1	C_β-H_β in β-*O*-4′ substructures linked to a S unit (erythro) (A)
At_β(S)	86.7/4.0	C_β-H_β in β-*O*-4′ substructures linked to a S unit (threo) (A)
C_α	87.0/5.5*	C_α-H_α in β-5′ (phenylcoumaran) substructures (C)
$S_{2,6}$	104.3/6.7	$C_{2,6}$-$H_{2,6}$ in syringyl units (S)
$S'_{2,6}$	106.3 / 7.3	$C_{2,6}$-$H_{2,6}$ in C_α-oxidized (C_α=O) phenolic syringyl units (S′)
$S''_{2,6}$	106.8/7.2	$C_{2,6}$-$H_{2,6}$ in C_α-oxidized (C_αOOH) syringyl units (S″)
G_2	111.2/6.8 and 7.3	C_2-H_2 in guaiacyl units (G)
G_5	114.7/6.4 and 6.7	C_5-H_5 in guaiacyl units (G)
P_β	115.5/5.4	C_β-H_β in *p*-coumaroylated substructures (P)
$P_{3,5}$	115.7/6.8	$C_{3,5}$-$H_{3,5}$ in *p*-coumarate ester (P)
G_6	119.4/6.8	C_6-H_6 in guaiacyl units (G)
F_6	123.0/7.1	C_6-H_6 in ether-linked ferulic acid (F)
$P_{2,6}$	127.7/5.3	$C_{2,6}$-$H_{2,6}$ in *p*-hydroxyphenyl units (P)
$C'_{2,6}$	129.6/5.3	$C_{2,6}$-$H_{2,6}$ in conifery alcohol (C′)

*Too weak to be seen directly in Figure 7 but observable after increasing the intensity of HSQC NMR.

and β-1′ carbon-carbon linkages.

For a more complete structural characterization of TA lignin, the 2D NMR spectrum of fraction L_3 was analysed. The HSQC spectrum showed three regions corresponding to aliphatic, side chain and aromatic ^{13}C-^{1}H correlations. The aliphatic (nonoxygenated) region showed signals with no structural information and therefore is not discussed in detail. The oxygenated aliphatic (δ_c/δ_H 80-90/2.9 - 5.1 ppm) and the aromatic (δ_c/δ_H 98-135/5.2 - 7.6 ppm) regions of the HSQC spectrum are shown in Figure 7. The assignments of main lignin ^{13}C-^{1}H correlations of the HSQC spectrum are listed in Table 6, and the main substructures found in fraction L_3 are depicted in Figure 8. Signals from S and G units could be clearly observed in all of the spectra. Most of the spectra showed signals corresponding to β-*O*-4′ alkyl-aryl ether linkages. In the oxygenated aliphatic region of HSQC spectrum (Figure 7a), the C_γ-H_γ correlations in β-*O*-4′ linkages (substructure A, Figure 8) in fraction L_3 were observed at δ_c/δ_H 59.6/3.7 and 60.8/3.4 ppm. The signals for the C_γ-H_γ correlations in γ-acetylated lignin units (A′) can be observed at δ_c/δ_H 63.5/4.0 and 4.1 ppm, which undoubtedly demonstrates that this lignin is slightly acetylated and the acetylation takes place only at the γ-position of the lignin side chains. The C_α-H_α correlation in β-*O*-4′ substructures linked to a S unit was observed at δ_c/δ_H 72.2/4.9 ppm. The C_β-H_β correlation corresponding to the erythro and threo forms of the S-type β-*O*-4′ substructures can be distinguished at δ_c/δ_H 86.0/4.1 and 86.7/4.0 ppm, respectively (del Río et al., 2009). Signals of other lignin substructures were also observed in the HSQC spectrum of TA, and some of these signals correspond to minor structures. The structure of β-β′ (resinol) linkages (B) was observed with C_γ-H_γ at δ_c/δ_H 70.9/3.8 and 4.1 ppm, C_β-H_β at δ_c/δ_H 53.7/3.1 ppm, and C_α-H_α at δ_c/δ_H 85.1/4.7 ppm. The β-5′ (phenylcoumaran) structures (C) for the C_α-H_α correlation was observed at 87.0/5.5 ppm (Rencoret et al., 2009b). Besides, small signals with 60.1/3.2 and 81.3/5.09 ppm are probably indicative of traces of C_β-H_β and C_α-H_α in β-1′ (spirodienone) substructures (D). Other small signals for the C_γ-H_γ correlations were observed at 61.5/4.08 ppm in *p*-hydroxycinnamyl end groups (C′). The signal at δ_c/δ_H 55.9/3.8 ppm corresponds to the C-H correlation in methoxyls (del Río et al., 2009).

The main cross-signals in the aromatic region of the HSQC spectrum (Figure 7b) corresponded to the benzenic rings of the different lignin units. The S units give a signal for the $C_{2,6}$-$H_{2,6}$ correlation at δ_c/δ_H

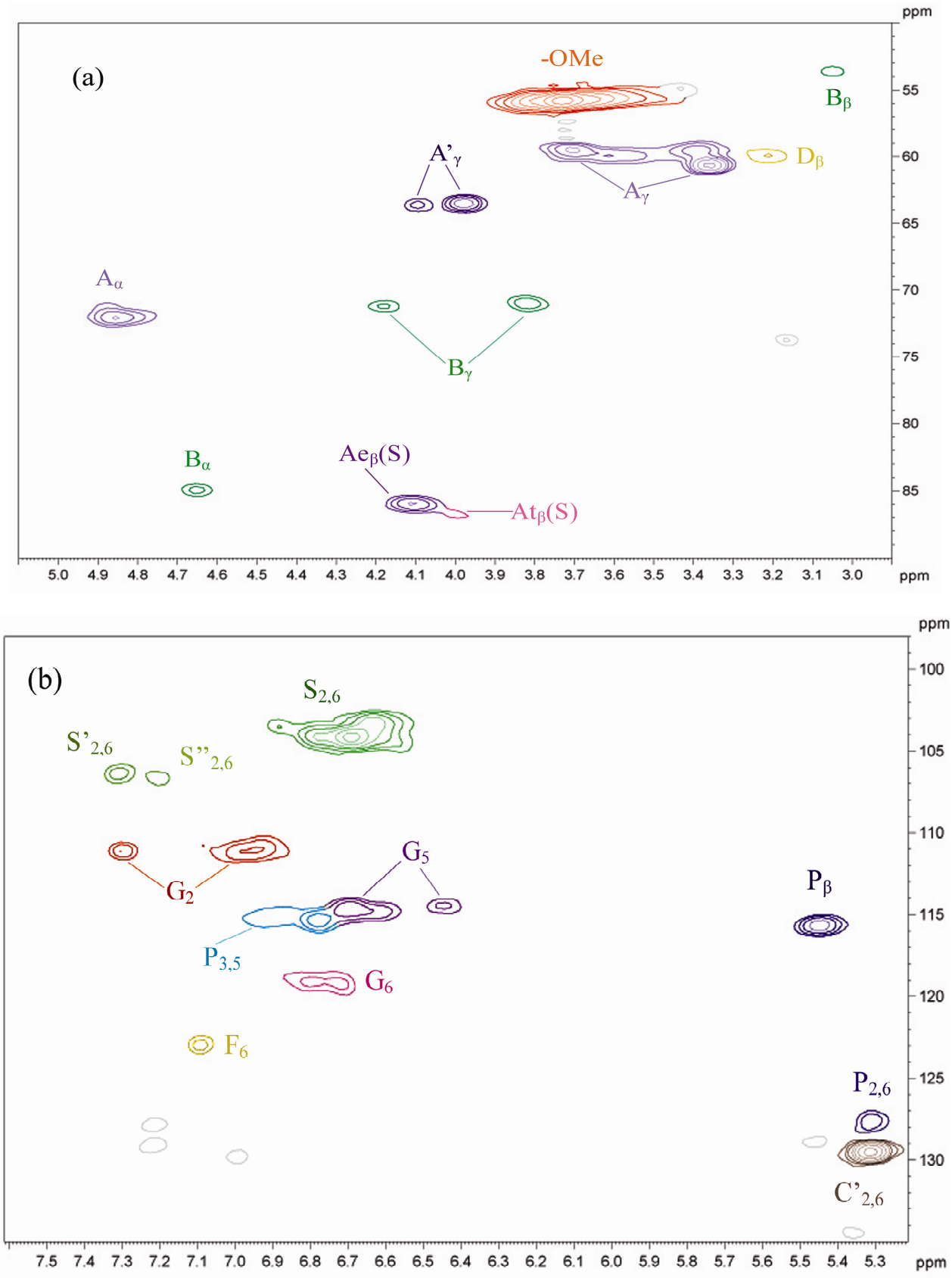

Figure 7a. HSQC NMR spectrum of lignin fraction L_3 isolated with 70% ethanol containing 0.5% NaOH from *Tamarix austromogoliac*: (a) oxygenated aliphatic region δ_c/δ_H 80-90/2.9-5.1 ppm, and (b) aromatic region δ_c/δ_H 98-135/5.2-7.6 ppm.

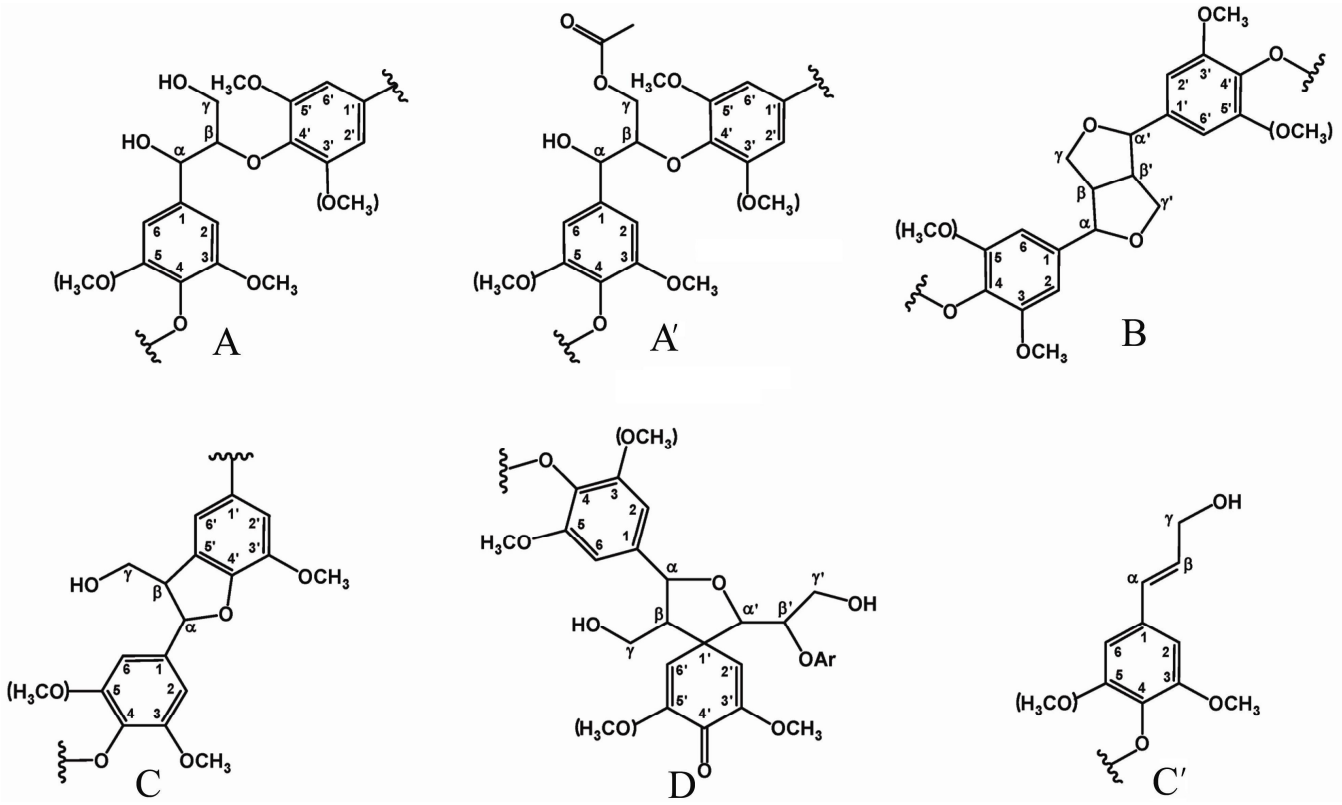

Figure 8. Main structures present in *T. austromogoliac* lignin: (A) β-*O*-4′ linkages; (A′) γ-acetylated β-*O*-4′ substructures; (B) resinol structures formed by β-β′/α-*O*-γ′/γ-*O*-α′ linkages; (C) phenylcoumarane structures formed by β-5′/α-*O*-4′ linkages; (D) spirodienone structures formed by β-1′/α-*O*-α′ linkages; (C′) *p*-hydroxycinnamyl alcohol end groups.

Table 7. Structural characteristics (relative abundance of the main inter-unit linkages) from integration of ^{13}C-^{1}H correlation signals in the HSQC spectrum of the fraction L_3 isolated from *T. austromogoliac*.

Inter-unit linkage	Linkage relative abundance (% of side chains involved)
β-*O*-4′ linked unies (A/A′)	73
Resinols (B)	19
Phenylcoumarans (C)	3
Spirodienones (D)	3
p-Hydroxycinnamyl alcohols (C′)	2

104.3/6.7 ppm, and the signals at 106.3/7.3 and 106.8/7.2 ppm represent $C_{2,6}$-$H_{2,6}$ in C_α-oxidized syringyl units (S′ and S″, respectively) (Ralph et al., 2004; Ibarra et al., 2007). G units were observed at C_2-H_2 (δ_c/ δ_H 111.2/6.8 and 7.3 ppm), C_5-H_5 (δ_c/δ_H 114.7/6.4 and 6.7 ppm) and C_6-H_6 (δ_c/δ_H 119.4/6.8 ppm) correlations. The double C_5-H_5 signal revealed some heterogeneity among the G units. This phenomenon is probably due to different substituents at C_4 (e.g., phenolic or etherified in different substructures) (Rencoret et al., 2009b). The signal at δ_c/δ_H 115.5/5.4 ppm was probably owning to C_β-H_β in *p*-coumaroylated substructures, while signal at δ_c/δ_H 115.7/6.8 ppm is originated from $C_{3,5}$-$H_{3,5}$ in *p*-coumarate ester. The $C_{2,6}$-$H_{2,6}$ correlation for the conifery alcohol give a signal at δ_c/δ_H 129.6/5.3 ppm (Capanema et al., 2001). Moreover, the H units give a signal for the $C_{2,6}$-$H_{2,6}$ correlation at δ_c/δ_H 127.7/5.3 ppm, and a signal at 123.0/7.1 ppm corresponds to C_6-H_6 correlation for ferulic acid ether structure. Signals at δ_c/δ_H 20.0 - 33.7/0.9 - 2.2 represent the C-H correlations of aliphatic as well as ethanol. The relative abundances of the main inter-unit linkages calculated from the HSQC spectrum (Table 7) indicated a predominance of β-*O*-4′ aryl ether linkages (73% of total side chains), followed by lower amounts of β-β′ resinol-type linkages (19% of total side chains), trace amounts of β-5′ phenylcoumaran (3%), β-1′ spirodienone-type substructures (3%) and cinnamyl end groups (2%).

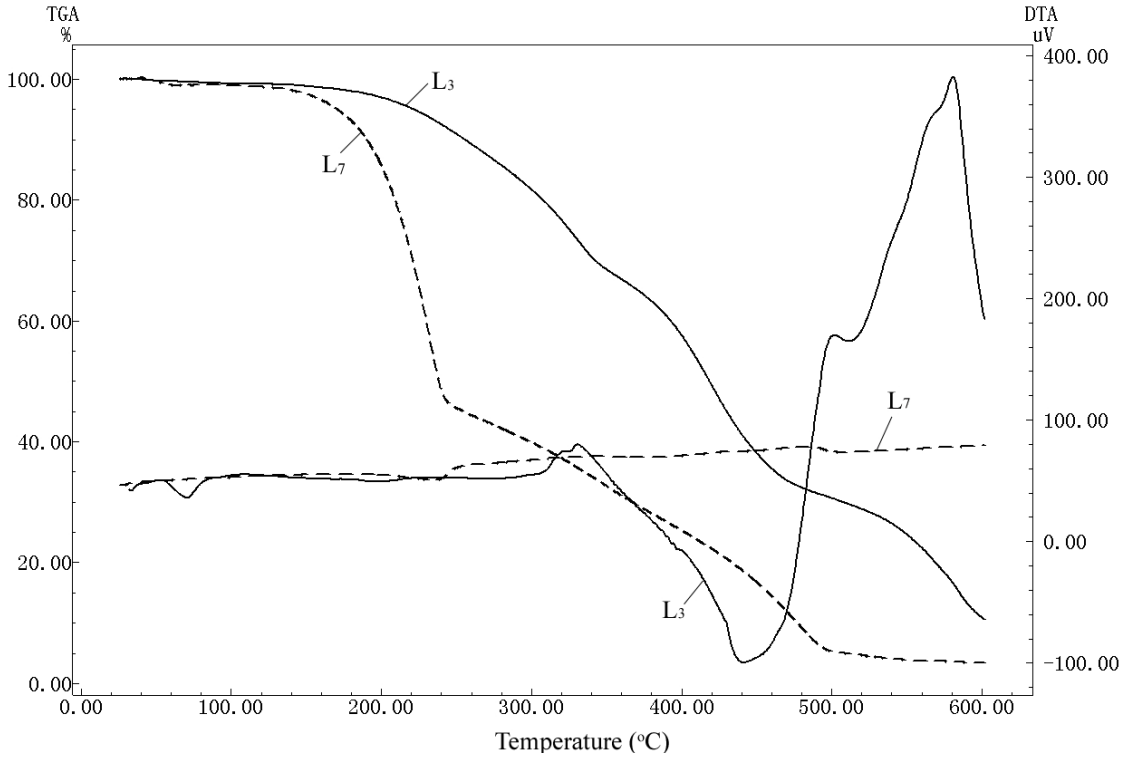

Figure 9. TGA/DTA curves of lignin fractions L_3 and L_7 isolated with 70% ethanol containing 0.5% NaOH at 70 ℃ for 5 h and 1 M $NH_3 \cdot H_2O$ at 50 ℃ for 5 h, respectively.

Thermal stability

TGA and DTA were used to study the thermal stability of the lignin isolated, Figure 9 gives thermograms of the acid-insoluble lignin fraction L_3 isolated with 70% ethanol containing 0.5% NaOH and fraction L_7 isolated with 1 M $NH_3 \cdot H_2O$. As can be seen from these curves, the decomposition process of lignin covered a larger temperature ranging from 200 - 500℃. The two lignin fractions of L_3 and L_7 began to decompose at 201 and 156℃, respectively. At 10% weight loss the decomposition temperature of fractions L_3 and L_7 started at 256 and 190℃, respectively. Similarly, at 50% weight loss the decomposition temperature of fractions L_3 and L_7 was observed at 418 and 238℃, respectively. These weight losses corresponded well with the lignin molecular weights given in Table 4, showing a decrease of thermal stability with a decrease in the molecular weight. It's clear that some quantities of carbon-carbon bonds between the lignin units are important, G-type units are able to form carbon-carbon bonds linkage by C-5 of the aromatic ring. These C-C bonds are not significantly cleaved during conditions such as treatment with alkali because of their higher stability. Therefore, we can conclude that lignins strictly composed of G units have a higher molecular weight compared to those having a higher content of S units.

The difference of the decomposition temperature at 10% weight loss of L_3 and L_7 was probably due to the low content (0.79%) of hemicelluloses in fraction L_3 than the content (5.74%) of hemicelluloses in fraction L_7, and the weight loss is due to the moisture present in the samples while the loss weight is attributable to carbon dioxide, carbon monoxide and evaporation of other pyrolysis products (Domínguez et al., 2008). Moreover, the decomposition process above 234℃ showed a maximum peal at -340℃, yielding mainly volatile products. In this stage, the main loss weight can be explained by the fact that lignin presents a complex structure made up of phenolic hydroxyl, carbonyl groups and benzylic hydroxyl (Yuan et al., 2009).

Conclusion

The treatment of dewaxed *T. austromogoliac* with DMSO, 70% ethanol containing 5% triethylamine, 70% ethanol containing 0.5% NaOH at 70℃ for 5 h and 1 M KOH, 1 M NaOH, 1 M LiOH and 1 M $NH_3 \cdot H_2O$ at 50℃ for 5 h released 61.7, 14.6, 27.4, 11.4, 11.2, 13.1 and 3.4% of the original lignin, respectively. A higher content of G units suggested that non-condensed β-aryl ether linked guaiacyl units are difficult to degrade than non-condensed β-aryl ether linked syringyl units in TA cell walls. The thermal stability of the lignin fractions showed a decreasing trend with decrease in molecular weight.

ACKNOWLEDGEMENTS

This work was supported by the grants from the Ministry of Science and Technology (973-2010CB732204), Natural Science Foundation of China (No. 30930073 and 30710103906), China Ministry of Education (No. 111, NCET-08-0728), State Forestry Administration (200804015, 948-2010-4-16) and Hei Long Jiang Province for Distinguished Young Scholars (JC200907).

REFERENCES

Billa E, Tollier MT, Monties B (1996). Characterisation of the monomeric composition of in situ wheat straw lignins by alkaline nitrobenzene oxidation: Effect of temperature and reaction time. J. Sci. Food Agric., 72: 250-256.

Boeriu CG, Bravo D, Gosselink RJA, van Dam JEG (2004). Characterisation of structure-dependent functional properties of lignin with infrared spectroscopy. Ind. Crops Prod., 20: 205-218.

Brunow G, Lundquis K, Gellerstedt G (1999). Lignin. In: Sjöström, E., Alén, R. (Eds.), Analytical Methods in Wood Chemistry, Pulping, and Papermaking. Springer-Verlag, Berlin, pp. 77-124.

Capanema BEA, Balakshin MY, Chen CL, Gratzl JS, Gracz H (2001). Structural analysis of residual and technical lignins by ^{1}H-^{13}C correlation 2D NMR-spectroscopy. Holzforschung, 55: 302-308.

del Río JC, Rencoret J, Marques G, Li J, Gellerstedt G, Jiménez-Barbero J, Martínez AT, Gutiérrez A (2009). Structural Characterization of the Lignin from Jute (*Corchorus capsularis*) Fibers. J. Agric. Food Chem., 57: 10271-10281.

Domínguez JC, Oliet M, Alonso MV, Gilarranz MA, Rodríguez F (2008). Thermal stability and pyrolysis kinetics of organosolv lignins obtained from *Eucalyptus globulus*. Ind. Crops Prod., 27: 150-156.

Faix O, Grunwald C, Beinhoff O (1992). Determination of phenolic hydroxyl group content of milled wood lignins (MWL's) from different botanical origins using selective aminolysis, FTIR, ^{1}H NMR and UV spectroscopy. Holzforschung, 46: 425-532.

Ibarra D, Chávez MI, Rencoret J, del Río JC, Gutiérrez A, Romero J (2007). Structural modification of eucalypt pulp lignin in atotally chlorine free bleaching sequence including a laccase-mediator stage. Holzforschung, 61: 634-646.

Izydorczyk MS, Biliaderis CG (1995). Cereal arabinoxylans: advances in structure and physicochemical properties. Carbohydr. Polym., 28: 33-48.

Lapierre C, Lallemand JY, Monties B (1982). Evidence of poplar lignin heterogeneity by combination of ^{13}C and ^{1}H NMR spectroscopy. Holzforschung, 36: 275-282.

Lawther JM, Sun RC, Banks WB (1995). Extraction, fractionation, and characterization of structural polysaccharides from wheat straw. J. Agric. Food Chem., 43: 667-675.

Marchessault RH, Coulombe S, Morikawa H, Robert D (1981). Characterization of aspen exploded lignin. Can. J. Chem. 60: 2372-2382.

Martínez AT, Rencoret J, Marques G, Gutiérrez A, Ibarra D, Jiménez-Barbero J, del Río JC (2008). Monolignol acylation and lignin structure in some nonwoody plants: a 2D NMR study. Phytochemistry, 69: 2831-2843.

Mohanty AK, Misra M, Drzal LT (2002). Sustainable bio-composites from renewable resources: Opportunities and challenges in the green materials world. J. Polym. Environ., 10: 19-26.

Nimz HH, Robert D, Faix O, Nemr M (1981). Carbon-13 NMR spectra of lignins, 8: structural differences between lignins of hardwood, softwoods, grasses and compression wood. Holzforschung, 35: 16-26.

Önnerud H, Gellerstedt G (2003). Inhomogeneities in chemical structure of hardwood lignins. Holzforschung, 57: 255-265.

Rakhmatullaev MS, Veksler NA, Smirnova LS, Abduazimov KA (1979). Nitrobenzene oxidation of fractions of cotton-plant dioxane lignin. Chem. Nat. Compd., 15: 66-68.

Ralph SA, Ralph J, Landucci L (2004). NMR database of lignin and cell wall model compounds. US Forest Products Laboratory, Madison, WI. Available online at http://ars.usda.gov/Services/docs.htm?docid=10491. (accessed July 2006).

Rencoret J, Marques G., Gutiérrez A, Nieto L, Jiménez-Barbero J, Martínez AT, del Río JC (2009a). Isolation and structural characterization of the milled-wood lignin from paulownia fortunei wood. Ind. Crops Prod., 30: 137-143.

Rencoret J, Marques G, Gutiérrez A, Nieto L, Santos JI, Jiménez-Barbero J, Martínez AT, del Río JC (2009b). HSQC-NMR analysis of lignin in woody (Eucalyptus globulis and Picea abies) and non-woody (Agave sisalana) ball-milled plant materials at the gel state. Holzforschung, 63: 691-698.

Saïdana D, Mahjoub MA, Boussaada O, Chriaa J, Chéraif I, Daami M, Mighri Z, Helal AN (2008). Chemical composition and antimicrobial activity of volatile compounds of *Tamarix boveana* (Tamaricaceae). Microbiol. Res., 163: 445-455.

Scalbert A, Monties B, Guittet E, Lallemand JY (1986). Comparision of wheat straw lignin preparations. I. Chemical and spectroscopic characterizations. Holzforschung, 40: 119-129.

Scalbert A, Monties B, Lallemand JY, Guittet E, Rolando C (1985). Ether linkage between phenolic acids and lignin fractions from wheat straw. Phytochemistry, 24: 1359-1362.

Sederoff RR, MacKay JJ, Ralph J, Hatfield RD (1999). Unexpected variation in lignin. Curr. Opin. Plant Biol., 2: 145-152.

Sun RC, Lawther JM, Banks WB (1997). Fractional isolation and physico-chemical characterization of alkali-soluble lignins from wheat straw. Holzforschung, 51: 244-250.

Sun RC, Lu Q, Sun XF (2001). Physico-chemical and thermal characterization of lignins from *Caligonum monogoliacum* and *Tamarix spp*. Polym. Degrad. Stabil., 72: 229-238.

Sun RC, Tomkinson J, Jones GL (2000a). Fractional characterization of ash-AQ lignin by successive extraction with organic solvents from oil palm EFB fibre. Polym. Degrad. Stabil., 68: 111-119.

Sun RC, Tomkinson J, Zhu W, Wang SQ (2000b). Delignification of maize stems by peroxymonosulfuric acid, peroxyformic acid, peracetic acid, and hydrogen peroxide. 1. Physicochemical and structural characterization of the solubilized lignins. J. Agric. Food Chem., 48: 1253-1262.

Sun XF, Sun RC, Fowler P, Baird MS (2005). Extraction and characterization of original lignin and hemicelluloses from wheat straw. J. Agric. Food Chem., 53: 860-870.

Tai DS, Terazawa M, Chen CL, Chang HM (1990). Lignin biodegradation products from birch wood by Phanerochaete chrysosporium. Holzforschung 44: 185-190.

Tejado A, Pena C, Labidi J, Echeverria JM, Mondragon I (2007). Physico-chemical characterization of lignins from different sources for use in phenol–formaldehyde resin synthesis. Bioresour. Technol., 98: 1655-1663.

Xu F, Sun JX, Sun RC, Fowler P, Baird MS (2006). Comparative study of organosolv lignins from wheat straw. Ind. Crops Prod., 23: 180-193.

Xu F, Sun RC, Zhai MZ, Sun JX, Jiang JX, Zhao GJ (2008). Comparative study of three lignin fractions isolated from mild ball-milled *Tamarix austromogoliac* and *Caragana sepium*. J. Appl. Polym. Sci., 108: 1158-1168.

Yuan TQ, He J, Xu F, Sun RC (2009). Fractional and physico-chemical analysis of degraded lignins from the black liquor of *Eucalyptus pellita* KP-AQ pulping. Polym. Degrad. Stabil., 94: 1142-1150.

Zhang DY, Pan BR, Yin LK (2003). The photogeographical studies of *Tamarix* (tamaricaceae). Acta Botanica Yunnanica, 25: 415-427.

Zhang KB, Zhao KG (1989). Affforestation for sand fixation in china. J. Arid Environ., 16: 3-11.

Zhang LM, Gellerstedt G (2007). Quantitative 2D HSQC NMR determination of polymer structures by selecting suitable internal standard references. Magn. Reson. Chem., 45: 37-45.